Modeling the nonlinear vibration response of a cracked rotor by Time Delay and Embedding Technique

ALFAYO A ALUGONGO
Department of Mechanical and Industrial Engineering
University of South Africa
P.O. Box Private Bag x06, Florida, 1710
REPUBLIC OF SOUTH AFRICA
alugoaa@unisa.ac.za, http://www.unisa.ac.za

Abstract: -In this paper, a non-linear model for a cracked rotor is established based on constitutive equations and local flexibility due to a transverse breathing crack on a rotor shaft. The crack is characterized by a switching function and change in shaft stiffness, whose variation and value defines the closing-opening or breathing condition of the crack during rotation of the shaft. The model accounts for the rotor shaft weakening parallel and perpendicular to the direction of the crack opening. The system equation bears discontinuity, and its numerical solution exhibits bifurcation and chaos. The model is used to investigate the dynamics of the vibrating rotor system, and the crack force reconstructed' by Time delay and Embedding Technique. The crack force manifests the action of the crack on the rotor. It is observed that the largest computed Lyapunov exponent of the simulated time series is a good and sufficient indicator of the system's chaotic state. Various scenarios of the system at sub-critical and super-critical speeds have been simulated and discussed.

Key-Words: - Bifurcation, Chaos, Lyapunov exponent, Cracked rotor dynamics, Switching function

1 Introduction

Nomenclature

B	4×1 matrix
C, d	A damping matrix in ξ and η direction
G, e	Gyroscopic matrix and eccentricity respectively
h_a, h_b	Crack compliance in ξ and η direction respectively
k_ξ, k_η	Stiffness in ξ and η direction respectively
M	Equivalent mass of the rotor
Ω	Angular speed , $f = \Omega / 2\pi$
f	Rotating frequency
F_ξ	Elastic force in the direction of the rotating coordinate ξ
F_η	Elastic force in the direction of the rotating coordinate η
β	Angle between unbalance and crack opening directions
$\xi\ \eta$	Rotating coordinate parallel and perpendicular to the crack respectively.
K, k_o	System stiffness matrix and stiffness of the uncracked rotor respectively
$\Delta k_1, \Delta k_2$	Stiffness decrease in ξ and η direction respectively
x, y	Inertial coordinates axes

Wauer [1], Gasch [2] and Dimarogonas [3] have presented reviews on linear models used in cracked rotor dynamics. Dimarogonas and Papadopoulos [4, 5] proposed novel techniques for computing crack compliance which form a basis for various crack identification methods. Gasch's [6] dynamic model has stimulated evaluation of cracked rotors and consequent crack detection algorithms [7-8]. For a comparatively deep crack, the vibration of a rotor system exhibits nonlinear characteristics such as chaos and bifurcation [9-11]. In such a state, the crack opening-closing mechanism becomes elusive and unfeasible to yield the vibration response by analytical method. However, if damping between crack surfaces is neglected, then the crack breathing is solely dictated by stress in the crack's vicinity. In this condition and under tensional stress, the crack will be in an open state, and vice versa. For this scenario, the shaft distortion pattern will determine the open-closure state of the crack. Although the "Hinge-Mechanism" as is called,

may still be valid, the critical condition between opening and closing should be transformed into the displacement in body-fixed rotating coordinates $\xi-\eta$. In this paper, the nonlinear dynamics of a cracked De Laval rotor on stiff isotropic bearings (Fig.1) is investigated. The model is established for non-weight dominance, i.e. the static deflection is of small order magnitude in comparison to the dynamic deflection and the crack breathing is determined by vibration due to dynamic and static forces.

2 Cracked rotor model

Dimarogonas [4] has shown that, the compliance h, of a shaft in ξ and η directions will increase in case of an opening crack (fig.2). The additional compliance in η direction is usually neglected when the crack is shallow and the elastic force crack model equation sufficiently represented by

$$\begin{bmatrix}\xi\\ \eta\end{bmatrix}=\begin{bmatrix}h+h_a & 0\\ 0 & h\end{bmatrix}\begin{Bmatrix}F_\xi\\ F_\eta\end{Bmatrix} \tag{1}$$

in which case, the compliance in the crack direction only increases by a value h_a dependent on crack depth. For a nonlinear system, (which amounts to non weight-dominance), the additional compliance in η direction would cause considerable excitation in the vibration response. The elastic force crack model equation for this scenario takes the form

$$\begin{bmatrix}\xi\\ \eta\end{bmatrix}=\begin{bmatrix}h+h_a & 0\\ 0 & h+h_b\end{bmatrix}\begin{Bmatrix}F_\xi\\ F_\eta\end{Bmatrix} \tag{2}$$

The crack-opening condition would consistently formulated by considering curvature at the crack location. In a multi-degree of freedom (MDOF) rotor system, when the displacement in ξ direction and near the crack is larger than the displacement at the adjacent points, i.e.

$$\xi_i > \frac{\xi_{i-e_n}+\xi_{i+e_n}}{2} \tag{3}$$

the crack will be in an open state and vice versa. In a single degree of freedom (SDOF) rotor system, the vibration in the ξ direction would determine the crack-opening condition. For this case, if $f(\xi)$ is the crack switching function then,

$$f(\xi)=\begin{cases}1, & \xi>0\\ 0, & \xi<0\end{cases} \tag{4}$$

Consequently, the governing equation of a damped and non weight dominant cracked rotor system is

$$\begin{bmatrix}m & 0\\ 0 & m\end{bmatrix}\begin{Bmatrix}\ddot{\xi}\\ \ddot{\eta}\end{Bmatrix}+\begin{bmatrix}d & -2\Omega m\\ 2\Omega m & d\end{bmatrix}\begin{Bmatrix}\dot{\xi}\\ \dot{\eta}\end{Bmatrix}+\begin{bmatrix}k_\xi-\Omega^2 m & -d\Omega\\ d\Omega & k_\eta-\Omega^2 m\end{bmatrix}\begin{Bmatrix}\xi\\ \eta\end{Bmatrix}=\begin{Bmatrix}mg\cos(\Omega t)\\ -mg\sin(\Omega t)\end{Bmatrix}+em\Omega^2\begin{Bmatrix}\cos\beta\\ \sin\beta\end{Bmatrix} \tag{5}$$

where $k_\xi=k_o-f(\xi)\Delta k_1$ and $k_\eta=k_o-f(\xi)\Delta k_2$.

Eq. (5) is converted to a state space form to yield

$$\dot{z}=Az+u(t) \tag{6}$$

Where

$$A=\begin{bmatrix}0 & 1 & 0 & 0\\ -\frac{k_\xi}{m}+\Omega^2 & -\frac{d}{m} & 0 & 2\Omega\\ 0 & 0 & 0 & 1\\ -2\Omega & -\frac{k_\eta}{m}+\Omega^2 & 0 & -\frac{d}{m}\end{bmatrix} \tag{7}$$

$$z=[\xi,\dot{\xi},\eta,\dot{\eta}]' \tag{8}$$

The state vector q in inertial coordinates is established by the transformation

$$q=P\times z \tag{9}$$

Where

$$q=[x,\dot{x},y,\dot{y}]' \tag{10}$$

$$P=\begin{bmatrix}\cos(\Omega t) & 0 & -\sin(\Omega t) & 0\\ -\Omega\times\sin(\Omega t) & \cos(\Omega t) & -\Omega\times\cos(\Omega t) & -\sin(\Omega t)\\ \sin(\Omega t) & 0 & \cos(\Omega t) & 0\\ \Omega\times\cos(\Omega t) & \sin(\Omega t) & -\Omega\times\sin(\Omega t) & \cos(\Omega t)\end{bmatrix} \tag{11}$$

P is a transformation matrix. The state vector $z(k)$ is determined numerically from Eq.(6) leading to $q(k)$. The change in stiffness of the cracked shaft is a function of shaft vibration displacement response and rotating angle. Let the equation of motion of the cracked rotor system be of the form

$$M\ddot{\phi}(t)+(C+G)\dot{\phi}(t)+K(t,\phi)\phi(t)=f(t) \quad (12)$$

and consider the uncracked rotor under action of the crack as a system with an external excitation [6] in the form

$$M\ddot{\phi}(t)+(C+G)\dot{\phi}(t)+K\phi(t)=f(t)+N(\phi,t) \quad (13)$$

$$\phi=[x,y]' \quad (14)$$

where $N(z,t)$ is a nonlinear force. Let the two systems in eq (12) and eq (13) be equivalent. Ignoring gyroscopic term, eq.(13) in state space form will read

$$\dot{q}(t)=A_0 q(t)+Bu(t) \quad (15)$$

where

$$A_0=\begin{bmatrix} 0 & 1 & 0 & 0 \\ -\frac{k_0}{m} & -\frac{d}{m} & 0 & 0 \\ 0 & 0 & 0 & 1 \\ 0 & 0 & -\frac{k_0}{m} & -\frac{d}{m} \end{bmatrix} \quad (16)$$

By a suitable discretization interval l, the continuous system would be discretized into

$$q[(k+1)l]=e^{A_0 l}q[kl]+\int_0^l \frac{t}{T}e^{At}dt\times u[kl]+ \left(\int_0^l e^{A_0 l}dt-\int_0^l \frac{t}{T}e^{At}dt\right)u[(k+1)] \quad (17)$$

The sequence of the external force $u[k]$ may then be computed recursively by the equation

$$u[k+1]=\left(\int_0^l e^{At}dt-\int_0^l \frac{t}{T}e^{At}dt\right)^{-1}\times \left\{q[k+1]-e^{A_0 l}q[k]-\int_0^l \frac{t}{T}e^{At}dt\times u[k]\right\} \quad (18)$$

eq.(18) may as well be discretized approximately into

$$q[(k+1)l]=e^{A_0 l}q[kl]+\int_0^l e^{A_0 l}dt\cdot Bu[kl] \quad (19)$$

and

$$u[k]=\left[\int_0^l e^{A_0 l}dt\cdot B\right]^{-1}\left(q[k+1]-e^{A_0 l}q[k]\right) \quad (20a)$$

The state vector $q(k)$ is obtainable by numerical method. Only $u[k]$ in eq. (18) and eq.(20) are unknown whereas, $u[k]$ is computed from eq.(18) given the initial value evaluated from eq.(20). The "Crack force" is reconstructed discarding unbalance force from $u[k]$ and, a unique relation between the vibration responses and the "crack force" obtained as a crack detection tool. From the foregoing discussion, together with manipulation of eq.15 as a series based on variable *hk* instead of t, the system state and acceleration may be represented in the following form upon making vector u the subject:

$$u[kh]=B^{-1}\{\dot{q}[kh]-A\cdot q[kh]\} \quad (20b)$$

Further, exponential operation on A could be avoided by using eq. (20b) to rebuild $u[k]$, though, this requires prior designation of the acceleration sequence. An accurate reconstruction based on a practical rotor response is complicated by noise contamination. Prior noise elimination is imperative besides, l is to be reasonably small to curb on recursion errors.

2.1 Characterization of the rotor

The opening-closing function proposed by Gasch holds under weight dominance. For a weight-dominant vibration, the amplitude is far less than static sag of the rotor and breathing of the crack is determined by the rotation angle of the linear system. From the foregoing in conjunction with the "hinge-mechanism", the vibration response of the cracked rotor would be quasi-periodic.

When the rotating speed is larger than critical speed, the rotor will run at a super-critical speed, and in this case, the unbalance force dominates and determines the vibration of the cracked rotor. The angle between the crack and the unbalance directions determines the crack open-closure condition. In a stable vibration, the crack either will be opened or closed throughout. The vibration response of the cracked rotor will be periodic.

However, breathing becomes complex when the crack and unbalance forces become are of same order magnitude. In this condition, the system will neither be weight-dominant nor unbalance dominant. The response at given time values may become sensitive to crack parameters and rotating speed, leading to chaos.

From bifurcation plots, one may not uniquely distinguish quasi-periodic from chaotic vibrations. Based on the existing simulations, a rule of thumb is that, if the Poincare section is composed of discrete points, the vibration is

periodic, if it is a closed curve, the vibration is quasi-periodic, and if it is a fractal map, the vibration is chaotic. Precisely, Lyapunov exponent indicates chaos in the system and will be discussed in section 5. Whether chaos and bifurcation will appear or not depends on specific conditions.

In the current simulations, bifurcation and chaos are obvious for the changing parameter of rotation frequency as shown in Fig. 3, (where $a/D=0.5, e=2\times10^{-4}\ mm, d=200$) and Fig. 4, (where $a/D=0.4$, $e=2\times10^{-4}\ mm$, $d=100$). Similar results are depicted in Figs.5 and Fig.6. Bifurcation plots with respect to crack depth at $f=20\ Hz$, $e=0.05\ mm$ and $d=100$ are shown in Figs. 7 and. 8. Double and triple period Bifurcation is evident. The rotor orbit, power spectrum and Poincare sections are shown in Figs. 9-12 for a crack depth $a/D=0.2$. In fig 9c, the Poincare section is a single point, and the response is periodic. When $a/D=0.36$, the possibility of chaos is observed in Fig. 4. The rotor orbit is shown in Fig. 10a and the Poincare section in Fig. 10c depicts Chaos. The rotor orbit, power spectrum, Poincare sections are shown in Figs. 11 and 12 for values $a/D=0.44$ and $a/D=0.48$ respectively. Poincare sections change remarkably with the parameters and a consistent crack feature is not discernable. In Figs. 9b, 10b, 11b and 12b, the results are close to the power spectrum of a weight dominant rotor; emergence of high order harmonics is prevalent in the power spectrum if a crack exists. Unfortunately, these features cannot be used to diagnose an inchoate crack as they do not exist for a shallow crack.

.

2.1.1 Reconstruction of the dynamic measure of the crack

The 'crack force' is associated with the dynamic change of the crack and manifests excitation of the rotor by the crack. Its reconstruction is based on eqs. (19) - (20). For $a/D=0.1$, $m=25\ kg$ and $e=0.05\ mm$, the corresponding static sag is $u_o=mg/k_o=4.9\times10^{-2}\ mm$ and the displacement due to the unbalance is $me\omega^2/k_o=9.87\times10^{-4}mm$. The corresponding static sag is larger than the vibration amplitude consequently, the rotor is weight dominant. Its reconstructed crack force is illustrated in fig. 13. The result is consistent with Gasch's hinge model except for high order harmonic components. Crack forces are about zero as the crack closes and change to periodic excitations as it opens. In fig.14, the crack forces are for $a/D=0.05$, apparently, a shallow crack. At $a/D=0.44$, $e=0.2mm$, $f=20Hz$, the system is chaotic and the force is shown in fig. 15. The crack force is of diversified frequency components. The reconstructed "crack force" bears a close relation to the crack behavior.

.

3 The Lyapunov Exponent

Lyapunov spectrum provides an intuitive description of the dynamic behaviour of a chaotic system. It quantifies the average rate of convergence or divergence of nearby trajectories in a global sense. Positive and negative Lyapunov exponent implies respectively divergence, and convergence. Consequently, a system with positive exponents has positive entropy, trajectories initially close move apart over time. The more positive the exponent, the faster the trajectories diverge. Similarly, for negative exponents, the trajectories move close to each other. A system with both positive and negative Lyapunov exponents is said to be chaotic. Based on the system's differential equations, Lyapunov spectrum is given by,

$$\lambda_i=\lim_{n\to\infty}\frac{1}{n}\ln\left(eig\prod_{p\to1}^{n}J(p)\right) \qquad (21)$$

where J is the system Jacobian as p moves around the attractor.

The crack breathes irregularly; the differential equations are discontinuous and eq. (21) is not directly adaptable for evaluation of Lyapunov exponents. Instead, $q(k)$ from eq. (15) has been treated as a noise-free signal and the system's largest Lyapunov exponent evaluated from it following Wolf et al [12] and Banbrook et al [13]. By Time Delay and Embedding [14], a new state space is established on the series calculated from equation (9).

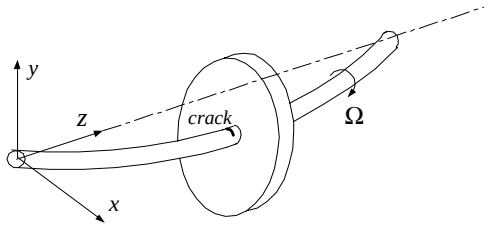

Fig.1 The De Laval rotor

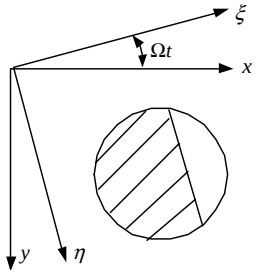

Fig.2 The rotating and inertial coordinates

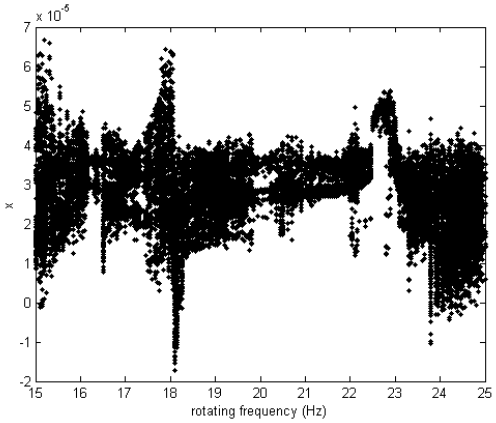

Fig. 3. The bifurcation diagram a/D=0.5;d=200; e=0.0002

For brevity, only results are given here. Wolf's approach was initiated by carrying out an exhaustive search of the data in the reconstructed state space to locate the nearest neighbor to the first point. Time delay was determined by the method proposed by Kember and Fowler [15]. Reconstructed attractors are

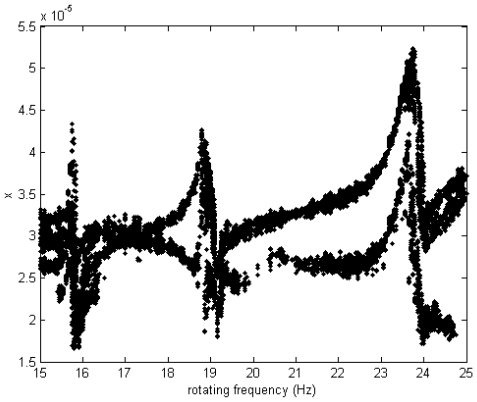

Fig. 4.The bifurcation diagram a/D=0.4; d=100; e=0.0002.

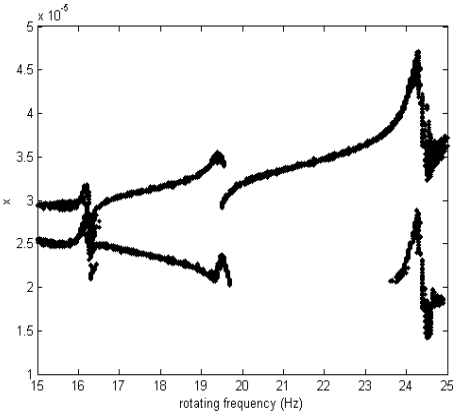

Fig. 5. the bifurcation diagram a/D=0.3; d=100; e=0.0002.

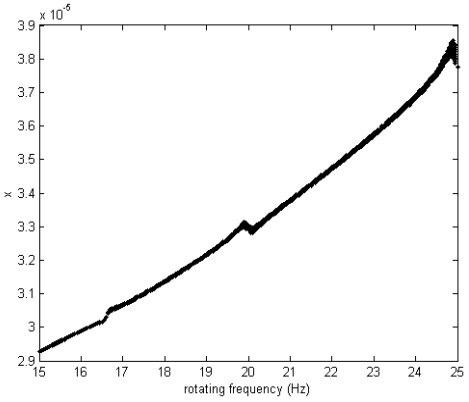

Fig. 6. the bifurcation diagram a/D=0.1; d=100, e=0.0002.

shown in figs. 16 and 17. The original attractors are illustrated in fig.9a and fig.10a respectively for the parameters $a/D = 0.36$, $e = 0.2\ mm$, $d = 100$, $f = 20\ Hz$.

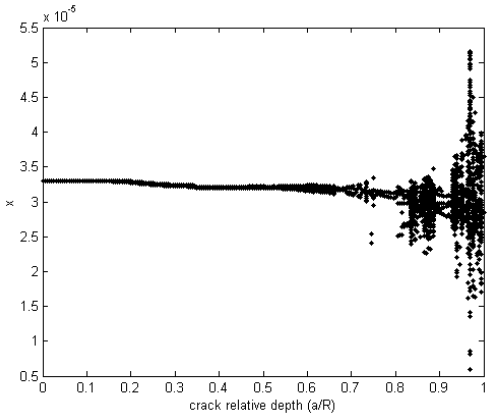

Fig. 7. The bifurcation diagram. Rotating frequency=20Hz, d=100, e=0.0002.

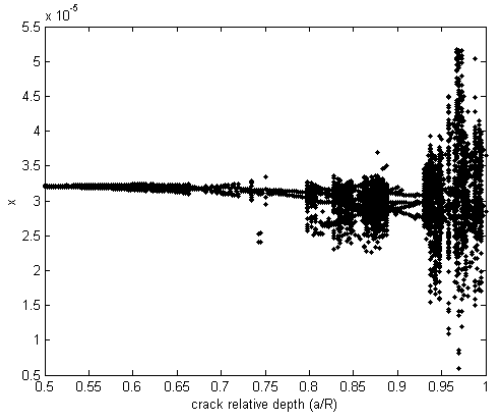

Fig. 8. The bifurcation diagram. Rotating frequency=20Hz, d=100, e=0.0002.

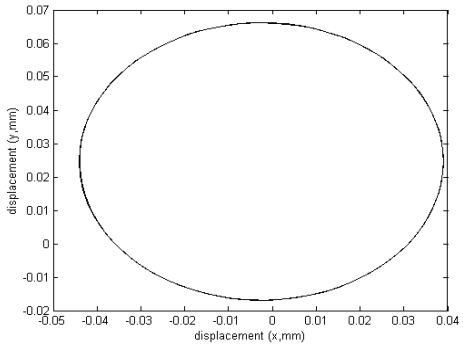

Fig. 9a. Rotor orbit .

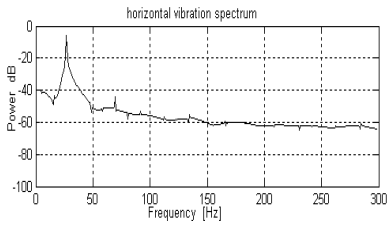

Fig 9b(i) horizontal vibration power spectrum

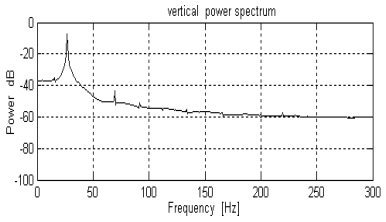

Fig. 9b(ii). Power spectrum.

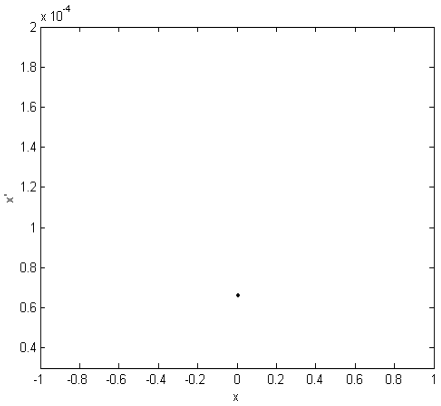

Fig. 9c. Poincare section.

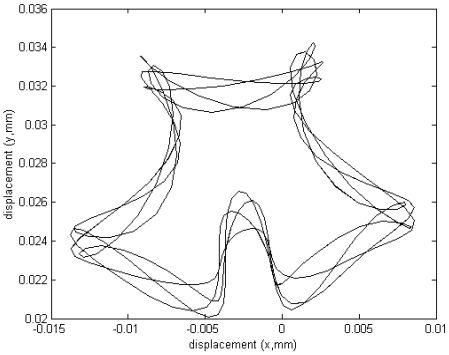

Fig. 10a. Rotor orbit.

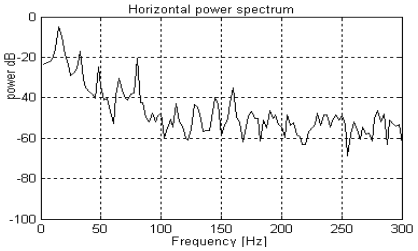

Fig. 10b(i). Power spectrum.

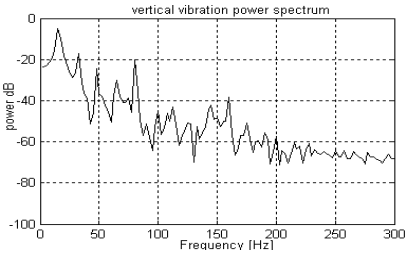

Fig. 10b(ii). Power spectrum.

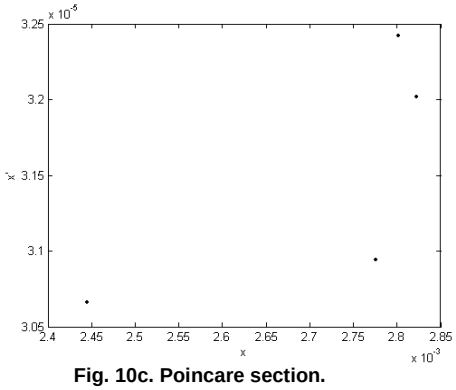

Fig. 10c. Poincare section.

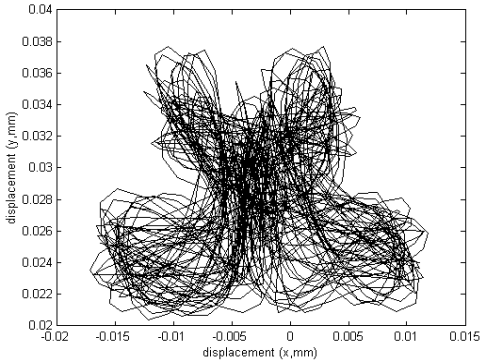

Fig. 11a. Rotor orbit.

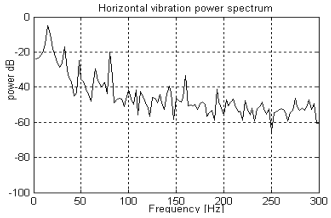

Fig. 11b(i). power spectrum.

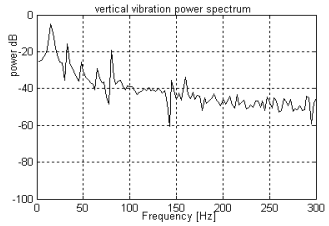

Fig. 11b(ii). Power spectrum.

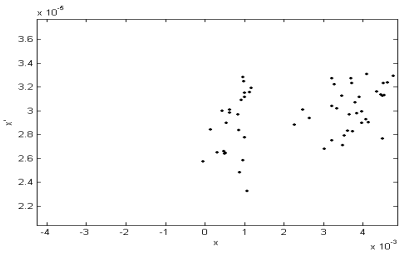

Fig. 11c. Poincare section.

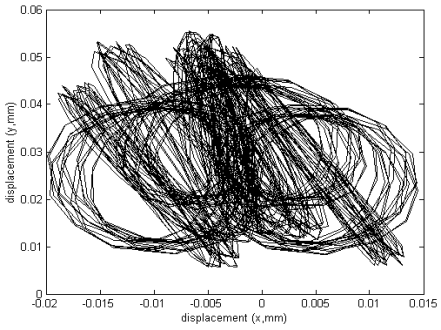

Fig. 12a. Orbit of rotor.

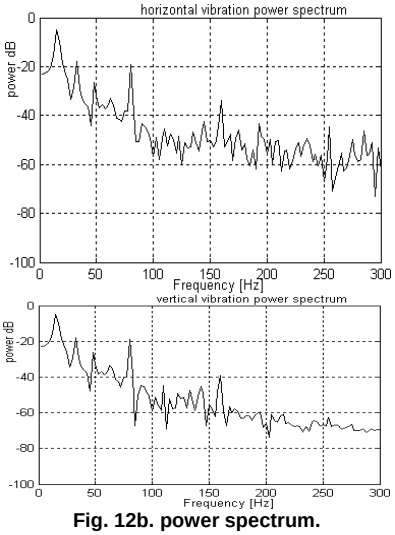

Fig. 12b. power spectrum.

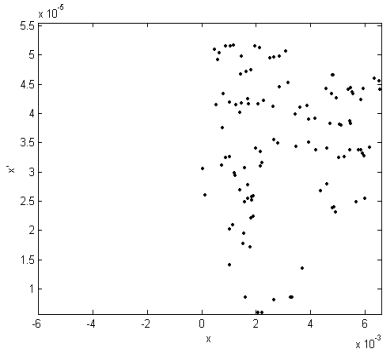

Fig. 12c. Poincare section.

The rotor orbit, power spectrum and Poincare plots are in fig. 10, and the vibration is

periodic; the largest Lyapunov exponent is convergent to zero (fig. 19). When $a/D = 0.48$ (orbit shown in fig. 12a), the largest Lyapunov exponent is convergent to a positive value (fig.20) signifying loss of stability.

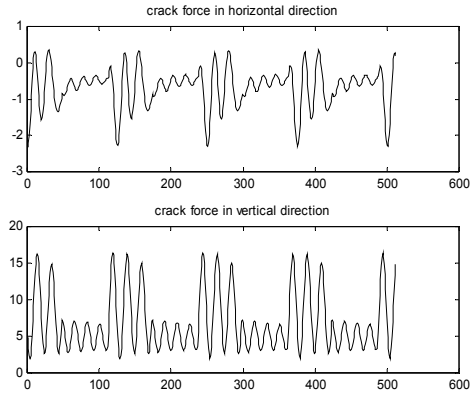

Fig. 13. Reconstructed crack forces.

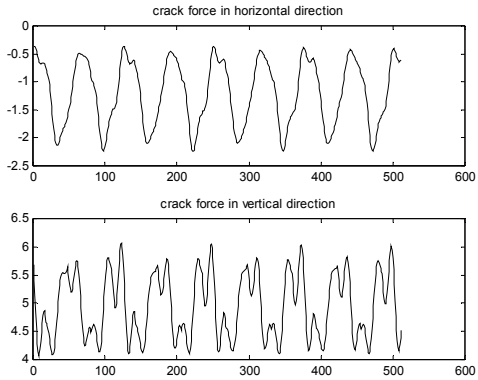

Fig. 14. Reconstructed crack forces.

4 Conclusion

A new technique based on state space theory and Time Embedding technique has been used to reconstruct the non-linear dynamics of a cracked rotor. The model used for the crack accounts for stiffness decrease in ξ and η directions respectively. The system is sensitive to rotation frequency and crack depth. Chaos and Bifurcation are observed as parameters fall into specific zones. It is demonstrated that the largest computed Lyapunov exponent of the simulated time series

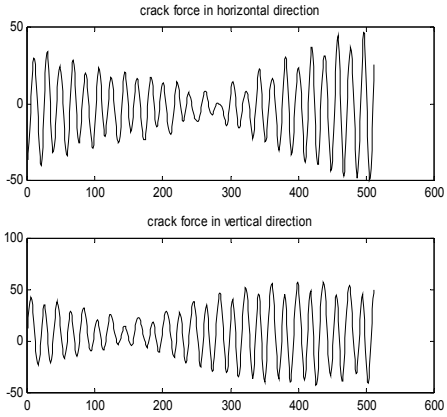

Fig. 15. Reconstructed crack forces.

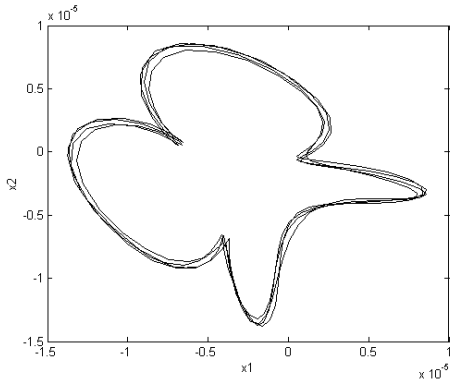

Fig. 16 Reconstructed attractor.

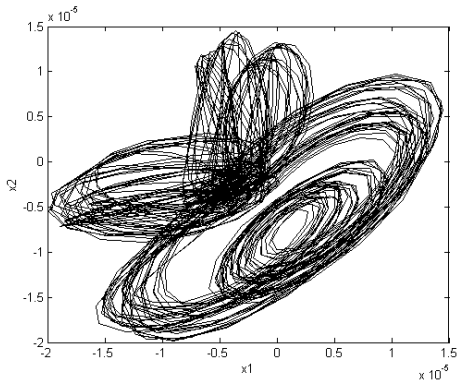

Fig. 17 Reconstructed attractor.

is a sufficient indicator for the system's chaotic state. The crack affects the rotor vibration in diversified modes dependent on the selected parameters. High order harmonics are an inherent crack symptom whether the model is weight dominant or non-weight dominant. The current result compares well with listed literature.

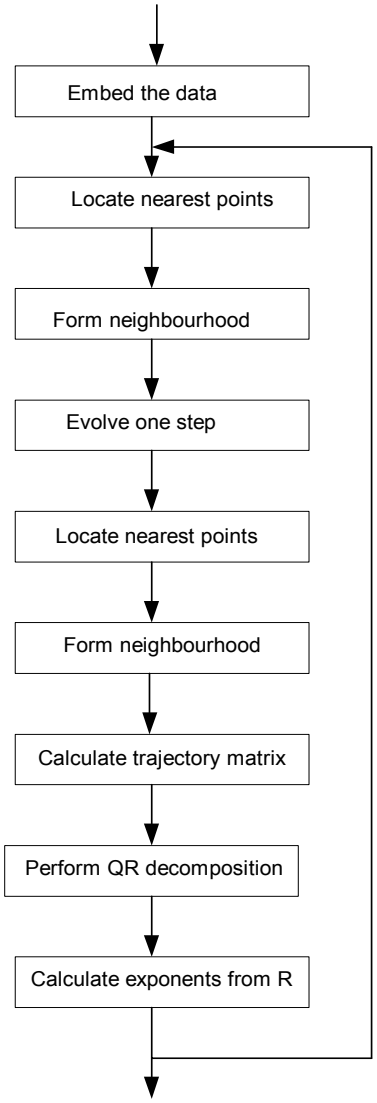

Fig.18 Overview of the algorithm for computing the system Lyapunov exponents

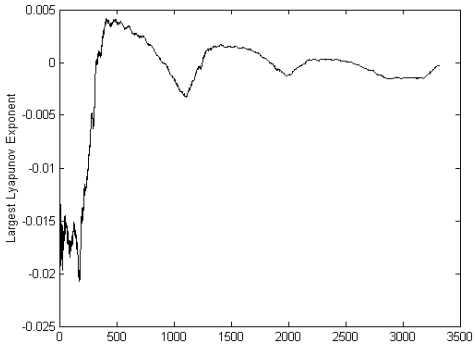

Fig. 19. Largest Lyapunov exponent.

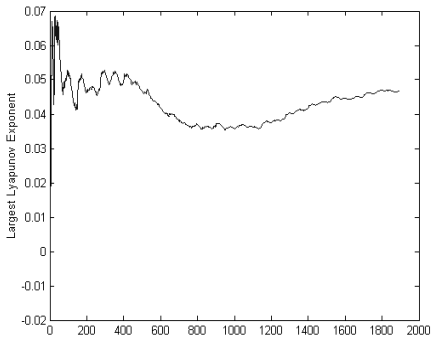

Fig. 20. Largest Lyapunov exponent

Acknowledgement

This research has been supported by the Dept of Mechanical and Industrial Engineering, University of South Africa.

References:

[1] Jorge Wauer, On the dynamics of cracked rotors: A literature survey, Applied Mechanics Reviews January, 1990, 43(1):13-17

[2] R.Gasch, A Survey of the Dynamic Behavior of a Simple Rotating Shaft with a Transverse Crack, Journal of Sound and Vibration, 1993, 160(2):313-332.

[3] A. D. Dimarogonas, Vibration of Cracked Structures: A State of the Art Review, Engineering Fracture Mechanics, 1996, 55,831-857.

[4] A.D.Dimarogonas and C.A.Papadopoulos, Non-linear Rotor Dynamics As Applied To Oilwell Drillstring Vibrations, Journal of Sound and Vibration, 1991, 147(1):115-135.

[5] C.A Ppdopoulos and A.D.Dimarogonas , Coupled longidutinal and bending vibrations of a rotating shaft with an open crack, Journal of Soumd and Vibration, 117(1):81-93

[6] R.Gasch, Dynamic behavior of a simple rotor with a cross-sectional crack, vibrations in Rotating Machinery, Institution of Mechanical Engineers, London, 1976,123-128.

[7] Mayes. I.W. and Davies. W.G.R, The Vibrational Behavior of a Rotating Shaft System Containing a Transverse Crack, Vibrations in Rotating Machinery, Institution

of Mechanical Engineers, London, 1976, 53-65.

[8] Grabowski B, The Vibrational Behavior of a Rotating Shaft Containing a Transverse Crack, Dynamics of Rotors-Stability and System Identification, CISM Courses and Lectures no 273, Springer, NewYork, 1984, 423-465.

[9] P.C.Müller, J.Bajkowski and D. Söffker, Chaotic Motions and Fault Detection in a Cracked Rotor, Nonlinear Dynamics, 1994, 5:233-254.

[10] A. Alugongo, C. Jin, Characterization and reconstruction of crack forces for a cracked De Laval rotor based on state space theory, ASME 2003 DETC2003/MECH-48582

[11] Jianhua Peng, Yanzhu Liu, Chaotic motion of a gyrostat with asymmetric rotor, International Journal of Non-Linear Mechanics, 2000(35):431-437.

[12] Alan Wolf, Jack B.Swinneh and John A.Vastano, Determining Lyapunov Exponents From a Times Series, Physica 16D, 1985, 285-317.

[13] M. Banbrook, G. Ushaw, and S. McLaughlin, How to Extract Lyapunov Exponents from Short and Noisy Time Series, IEEE Transactions on Signal Processing, May 1997, 45(5):1378-1382.

[14] F. Takens, Detecting Strange Attractors in Turbulence, in Lecture Notes in Mathematics, Springer, Berlin, 1981, (898):366-385.

[15] G. Kember and A. C. Fowler, A Correlation Function for Choosing Time Delay in Phase Reconstruction, Physical Letters A, 1993, 179,72-80.